

Cite this: *Phys. Chem. Chem. Phys.*, 2011, **13**, 15094–15102

www.rsc.org/pccp

PAPER

Structural characterization and DFT study of V^{IV}O(acac)₂ in imidazolium ionic liquids†

Andreia Mota,^a Jason P. Hallett,^b Maxim L. Kuznetsov^a and Isabel Correia^{*a}

Received 16th March 2011, Accepted 15th June 2011

DOI: 10.1039/c1cp20800d

We report the structural characterization of vanadyl acetylacetonate in imidazolium room temperature ionic liquids—bbimNTf₂, bmimNTf₂, C₃OmimNTf₂, bm₂imNTf₂, bmimPF₆, bmimOTf, bmimBF₄, bmimMeCO₂, bmimMeSO₄, bmimMe₂PO₄ and bmimN(CN)₂—and organic solvents. The complex was characterized by visible electronic (Vis) and EPR spectroscopies. VO(acac)₂ shows solvatochromism in the selected ionic liquids and behaves as in organic solvents, evidencing coordination of the ionic liquid anion in the solvents with higher coordinating ability. The Lewis basicity order obtained for the IL anions was: PF₆[−] < NTf₂[−] < OTf[−] ≈ MeCO₂[−] < MeSO₄[−] < BF₄[−] ≈ N(CN)₂[−] < Me₂PO₄[−]. The solvent effect on the spectroscopic data was tentatively examined using linear solvation energy relationships based on the Kamlet–Taft solvent scale (α , β and π^*), however no suitable correlation was found with all data. The EPR characterization showed the presence of two isomers in bmimOTf, bmimMeCO₂ and bmimMe₂PO₄, suggesting coordination of the ionic liquid anions in both equatorial and axial positions. The full geometry optimization of *cis*-/*trans*-VO(acac)₂(OTf)[−] and *cis*-/*trans*-VO(acac)₂(OTf)(mmim) structures was done at the B3P86/6-31G* level of theory. The calculations confirm that the anion OTf[−] is able to coordinate to VO(acac)₂ with the *trans* isomer being more stable than the *cis* by 4.8 kcal mol^{−1}.

Introduction

Room temperature ionic liquids are solvents composed entirely of ions.¹ Over more than a decade they have been attracting the attention of the scientific community due to their unique properties and applications. One of the many advantages of ionic liquids is the tunability of their solvent properties through the choice of a cation/anion combination.^{1,2} Different combinations lead to a huge number of ionic liquids with different properties. One of the most important fields of ionic liquids application is catalysis, in which the focus has been on how well the catalyst is retained in the ionic liquid phase and whether or not it can be recycled. Many times this implies modifications in the catalyst structure, however this does not mean that the modified catalyst will perform as well as the original one. Moreover, there is the question on which ionic liquid to choose in order to maximize the catalyst performance. While it is frequently assumed that ionic liquids are non-coordinating polar solvents, the ease with which the anion of the ionic liquid is displaced from the transition metal complex has been shown to be an important factor in the catalyst's performance.^{3,4}

So, understanding the behavior of transition metal ions in ionic liquids is a key issue in the determination of the process efficiency and it may lead to the development of more valuable systems.

It was initially thought that a highly polar medium like an ionic liquid, which consists of charged ions, would easily dissolve other salts. However, it has been shown that ordinary metal salts have sometimes very low solubility in many ionic liquids. Solvent–solute interactions take place at a molecular level and a variety of different interactions have to be taken into account. Solvent–solute interactions can be either specific or non-specific. Non-specific interactions are dipole forces (dispersion, London, induction or Debye, orientation or Keesom forces) and ion/dipole forces (Coulomb forces). Specific interactions include hydrogen bond donor and/or hydrogen bond acceptor interactions, electron pair donor/electron pair acceptor or charge-transfer interactions, and solvophobic interactions (which can become important in highly structured solvents like ILs).⁵

The coordinating ability of an ionic liquid is a very important parameter if we consider a catalyst that has to coordinate to a substrate in order for a reaction to occur. This has been shown to depend on the anion.^{4,6} Several methods have been used to evaluate the coordination ability of ionic liquid anions, the simplest one being the measurement of the Vis spectra of solvatochromic dyes. Solvatochromic dyes are substances that are sensitive to specific and/or non-specific interactions with the solvent. Their electronic spectrum changes considerably with the solvent's polarity and several probes have been used

^a Centro Química Estrutural, Instituto Superior Técnico, TU Lisbon, Av. Rovisco Pais, 1049-001 Lisbon, Portugal.

E-mail: icorreia@ist.utl.pt

^b Chemistry Department, Imperial College London, London, SW7 2AZ, UK

† Electronic supplementary information (ESI) available. See DOI: 10.1039/c1cp20800d

to determine the interactions with ionic liquids, particularly transition metal complexes: $[\text{Fe}(\text{phen})_2(\text{CN})_2]\text{ClO}_4$,⁷ $[\text{Cu}(\text{acac})(\text{tmen})][\text{B}(\text{Ph})_4]$,^{4,6} $[\text{Ni}(\text{acac})(\text{tmen})][\text{B}(\text{Ph})_4]$ ⁸ and $[\text{Mn}(\text{NTf}_2)_2]$,⁹ are some examples.

The lowest energy d-d band of the square planar cation $[\text{Cu}(\text{acac})(\text{tmen})][\text{B}(\text{Ph})_4]$ {acac = acetylacetonate and tmen = *N,N,N',N'*-tetramethylethylenediamine, $\text{B}(\text{Ph})_4$ = tetraphenylphosphine} correlates well with solvent donor numbers.¹⁰ The observed shift results from the d-orbital splitting of copper(II) as the complex becomes five or six coordinated. The results for ionic liquids revealed that the spectroscopic shift was completely independent of the nature of the cation and was only dependent on the anion.⁶ The basicity order obtained for the IL anions was $\text{PF}_6^- < \text{NTf}_2^- < \text{OTf}^-$. With $[\text{Ni}(\text{acac})(\text{tmen})][\text{B}(\text{Ph})_4]$ again no substantial influence from the IL cation was observed,⁸ and the basicity order was: $\text{PF}_6^- < \text{BF}_4^- < \text{NTf}_2^- < \text{OTf}^- \ll \text{HCOO}^- \ll \text{DCA}^- \ll \text{TFA}^- \ll \text{PO}_2(\text{OEt})_2^- \ll \text{Cl}^-$, in agreement to the one obtained with the Cu^{2+} complex. The application of the d^5 transition metal complex $\text{Mn}(\text{NTf}_2)_2$ ⁹ resulted in the same basicity order.

A transition metal complex that has been applied as a catalyst in many organic reactions is $\text{VO}(\text{acac})_2$. Its properties have been studied by several researchers,^{11–17} and the crystal structure was published in 1962.¹⁸ In the solid state $\text{VO}(\text{acac})_2$ is five-coordinated; however, upon dissolution in organic solvents,

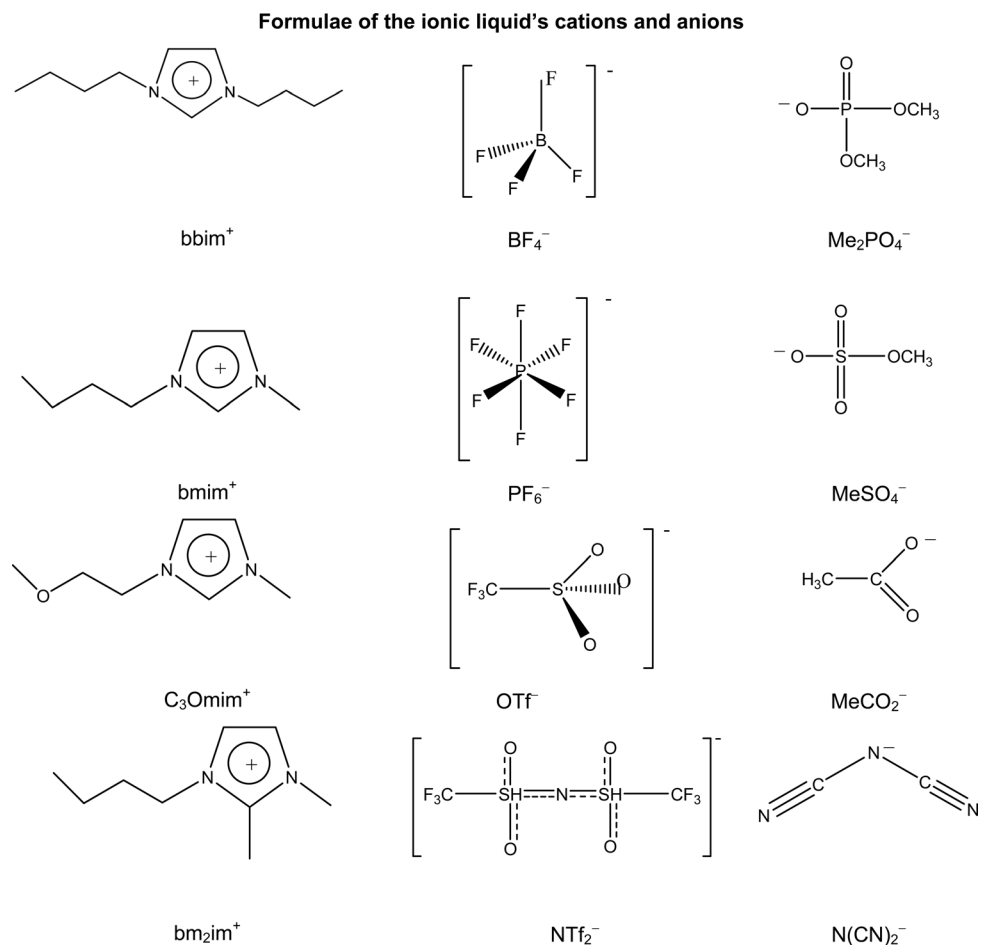
the vanadium may coordinate to a donor molecule in the vacant position, generating $[\text{VO}(\text{acac})_2\text{S}]$ (where S = solvent donor molecule). Several spectroscopic techniques have been employed to determine the coordination number, the geometry of the complex, and whether the incoming ligand is *trans* or *cis* to the oxo group.^{15,17,19,20} However, the literature is not in complete agreement since several authors propose equilibrium between *cis* and *trans* structures^{12,21} and others state that only the *trans* isomer is observed in solution.^{16,22}

In this report we use this transition metal complex to study the solvation process in ionic liquids, to evaluate the coordination of the ionic liquid anion, and the existence of specific and non-specific interactions. To do so, we will present spectroscopic studies in selected ionic liquids and organic solvents and the correlation of the spectroscopic data with solvent parameters. The solvent effect on the structure of the vanadium complex $\text{VO}(\text{acac})_2$ is examined using linear solvation energy relationships (LSER) based on the Kamlet–Taft solvent scale (α , β , and π^*).

Results and discussion

Characterization of the ionic liquids

The ionic liquids chosen for this study are depicted in Scheme 1. Syntheses of the ionic liquids were performed under



anaerobic conditions using standard Schlenk techniques. The preparations and spectral data of the ionic liquids have been described elsewhere²³ and are collected in the ESI.† The procedure used in their preparation and purification (washing with water, addition of charcoal, and filtration through alumina) afforded colorless liquids, suitable for spectroscopic studies. The analytic characterization showed the absence of impurities, such as residual chloride, which might change considerably their solvation properties. Before using the ILs were dried for at least 48 h under vacuum at 50 °C. The water content of the dried ionic liquids was measured by Karl Fischer coulometer analysis. For the hydrophobic ILs the values did not exceed 350 ppm but for the most hygroscopic they are *ca.* 1500 ppm, which in terms of water concentration corresponds to 0.08 M.

Solvatochromism in organic solvents

VO(acac)₂ has long been used as a solvatochromic probe.^{17,24} It is stable, soluble in a wide range of organic solvents and its visible absorption spectrum (*Vis*) is strongly solvent dependent. The five coordinated square pyramidal VO(acac)₂ may become six coordinated, with the addition of a solvent molecule in the axial position.^{24–27} The d–d absorption spectra of vanadyl complexes are interpreted considering C_{4v} symmetry for the square pyramid, and three transitions are expected, considering the following energy levels:²⁸

$$b_2(d_{xy}) < e(d_{xz}, d_{yz}) < b_1(d_{x^2-y^2}) < a_1(d_{z^2})$$

Since it is considered that b₂ is an almost pure vanadium 3d_{xy} orbital and e(d_{xz}, d_{yz}) is a combination of vanadium and oxygen orbitals, the lowest energy transition (λ_1)—from b₂(d_{xy}) to e(d_{xz}, d_{yz})—should be sensitive to axial perturbations from the solvent.²⁵

Table 1 Kamlet–Taft parameters for the ionic liquids used in this study

Ionic liquid	α	β	π^*
bmimPF ₆	0.63	0.21	1.03
bmimBF ₄	0.63	0.38	1.05
bmimOTf	0.63	0.46	1.01
bmimNTf ₂	0.62	0.24	0.98
C ₃ OmimNTf ₂	0.63	0.23	0.99
bm ₂ imNTf ₂	0.38	0.24	1.01
bmimN(CN) ₂	0.54	0.60	1.05
bmimMeCO ₂	0.47	1.20	0.97
bmimMeSO ₄	0.55	0.67	1.05
bmimMe ₂ PO ₄	0.45	1.12	0.97

Table 2 LSER fits for VO(acac)₂. LSER correlation coefficients $\nu_{\max,0}$, a , b and s of the Kamlet–Taft parameters α , β and π^* , respectively, with standard deviation (in brackets) and p -values (in square brackets); number of solvents (n), significance (F), coefficient of determination (R^2) and standard deviation (SD)

$\nu_{\max,0}$ (10 ⁻³ cm ⁻¹)	a	b	s	n	F	R^2	SD	Ref.
15.2 (±0.3) [6 × 10 ⁻¹⁴]	—	-2.8 (±0.5) [1 × 10 ⁻⁴]	—	12	1.4 × 10 ⁻⁴	0.781	0.427	This report—organic solvents
14.9 (±0.2) [4.0 × 10 ⁻¹⁶]	—	-2.8 (±0.4) [9.8 × 10 ⁻⁶]	—	13	9.8 × 10 ⁻⁶	0.827	0.307	24
14.8 (±0.2) [1.5 × 10 ⁻⁹]	—	-2.6 (±0.5) [0.002]	—	8	0.0017	0.796	0.394	37
14.8 (±0.2) [4.8 × 10 ⁻⁹]	-0.7 (±0.3) [0.05]	-2.1 (±0.4) [0.004]	—	8	0.0014	0.896	0.280	37
15.9 (±0.5) [6.7 × 10 ⁻⁵]	—	-4.3 (±1.0) [0.02]	—	5	0.024	0.809	0.459	25
14.0 (±0.4) [4.0 × 10 ⁻¹⁰]	—	-1.5 (±0.6) [0.04]	—	10	0.038	0.435	0.671	This report—ionic liquids

A particularly successful approach when attempting to quantitatively understand solvent-dependent data is the linear solvation energy relationship (LSER). One example is the equation, developed by Kamlet and Taft,^{29–32} which relates the variation of any solute property in terms of three solvent parameters (α , β and π^*). α is a quantitative scale of the hydrogen-bond acidity of a solvent, or its ability to donate a hydrogen bond; β is a scale of the hydrogen-bond basicity of a solvent, or its ability to accept a hydrogen bond; and π^* is the solvent dipolarity/polarizability, which is a scale of the ability of the solvent to stabilize a charge or dipole. Each of the parameters is empirically obtained and has been measured for a wide range of solvents, including ionic liquids. These scales have been used in multi-parameter equations to fit a number of different solvent-dependent observations, with the most useful form shown in eqn (1), where (XYZ)₀ is the intercept term which is the XYZ value in the absence of the solvent (*i.e.* the gas phase or a non-polar solvent).

$$XYZ = (XYZ)_0 + a\alpha + b\beta + \pi^* \quad (1)$$

This methodology was applied to our spectroscopic data and the Kamlet–Taft parameters determined previously for the ionic liquids and used in this study^{33–35} are reported in Table 1. For the organic solvents the parameters used were the ones published by Marcus.³⁶

The results of these LSER fits for the solvation of VO(acac)₂ in organic solvents (*ca.* 5 mM solutions), along with the associated statistical data, are shown in Table 2. We found that the wavenumber of the lowest energy transition decreases with β , the solvent basicity. The correlations made from data reported by other authors in the literature^{24,25,37} also show the same trend.

The LSER equations obtained in each case present good correlations and the p -values obtained for each coefficient show that they are statistically significant. However, the analysis of the data from Guzy *et al.*³⁷ shows that the inclusion of the solvent hydrogen-bond acidity, α , in the LSER equation increases considerably the fit. Comparison of the λ_1 obtained in the same solvent by different authors evidences the discrepancy in the collected data: *pe.* in benzene the values found were 683,²⁴ 671³⁷ and 660 nm,²⁵ the difference being 25 nm.

Solvatochromism in ionic liquids

Since one of our goals was to evaluate the behavior of the acetylacetonate vanadium complex in ionic liquids, the ILs were chosen in order to allow the comparison of cationic and

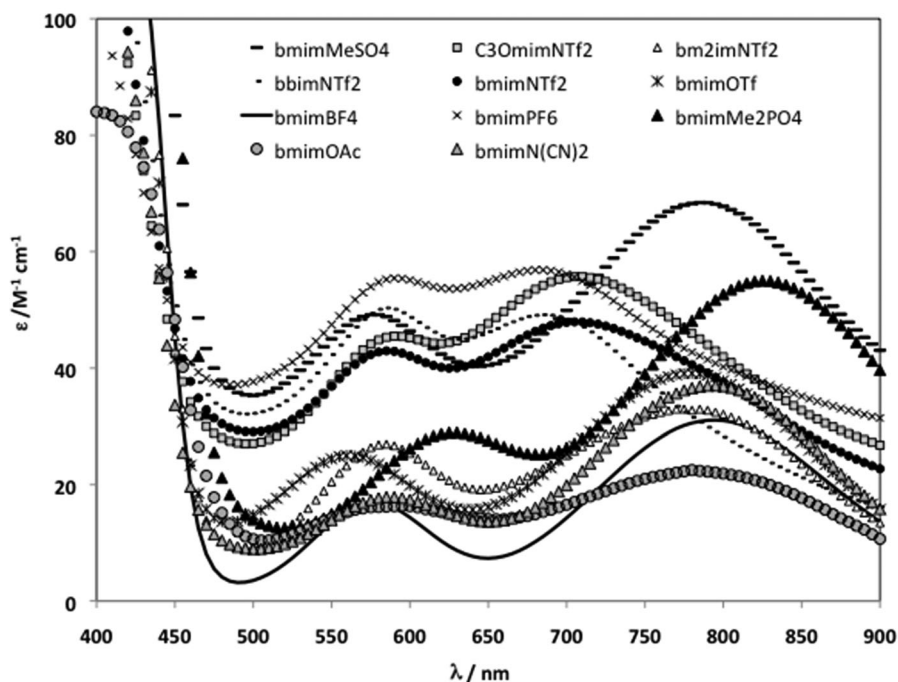


Fig. 1 Electronic absorption spectra of $\text{VO}(\text{acac})_2$ in the visible region measured in different ionic liquids.

anionic effects—several ILs contain the bmim cation and several contain the NTf_2 anion.

The spectra of $\text{VO}(\text{acac})_2$ in the different ionic liquids are shown in Fig. 1 and general spectroscopic data are collected in Table 3. Analysis of the data shows that $\text{VO}(\text{acac})_2$ is solvatochromic, with a shift in λ_1 of 143.5 nm when going from bmimPF_6 to $\text{bmimMe}_2\text{PO}_4$.

In most ionic liquids the complex shows three bands in the Vis range of the absorption spectra and axial symmetry in the EPR spectra. It has been proposed²² that a distortion from square planar towards a trigonal bipyramid geometry breaks the degeneracy of the $e(d_{xz}, d_{yz})$ orbitals resulting in the appearance of four bands in the Vis absorption spectra (bands I_a, I_b, II and III) and rhombicity in the EPR spectra of vanadyl compounds. The distortion of the geometry may be evaluated by analysis of the wavelength difference between the central transitions in the Vis spectrum, $|\lambda_{1b} - \lambda_2|$ and also by the difference between the EPR hyperfine coupling parameters $|A_x - A_y|$. The results suggest that (see Table 3) in bbimNTf_2 , bmimNTf_2 , bmimPF_6 , $\text{C}_3\text{OmimNTf}_2$ and $\text{bmimN}(\text{CN})_2$ there is a slight distortion of the geometry towards a trigonal bipyramid in the five-coordinated complex and in the other group of ILs the complex is six-coordinated and approaches an octahedral geometry. The metal–proton distances determined by ENDOR spectroscopy by Mustafi and Makinen¹⁶ for $\text{VO}(\text{acac})_2$ dissolved in methanol were best accounted for by a complex of square-pyramidal geometry, essentially identical to that determined by X-ray¹⁸ with a solvent molecule coordinated *trans* to the vanadyl oxygen and an axially positioned solvent molecule hydrogen-bonded to the vanadyl oxygen. We can therefore expect that solvents with high coordinating power will assume the same type of geometry as in methanol, presenting the same spectroscopic fingerprint.

The application of the LSER methodology with the Kamlet–Taft parameters determined for the ionic liquids (included in Table 1) did not provide a reasonable fit—see Table 2. However, the p -value obtained for the solvent basicity, β , is very low, showing that it is statistically relevant. The low value obtained for the correlation parameter R^2 may be due to uncertainties in the values determined for the β parameter for some ionic liquids, which depend on the dyes selection.

Overall, we can conclude that the solvation of $\text{VO}(\text{acac})_2$ in ionic liquids is similar to what occurs in organic solvents, in which the solvent basicity plays a dominant role. The other specific forces might be important but may be masked under the influence of this strong parameter.

In terms of anion basicity we can propose the following order, taking into account the energy of the lowest energy transition (λ_1): $\text{PF}_6^- < \text{NTf}_2^- < \text{OTf}^- \approx \text{MeCO}_2^- < \text{MeSO}_4^- < \text{BF}_4^- \approx \text{N}(\text{CN})_2^- < \text{Me}_2\text{PO}_4^-$. This is in agreement with the results obtained with the other transition metal complexes, except for BF_4^- .^{4,6,7,9} Since bmimBF_4 is the IL with the highest affinity for water, its different position on the basicity scale in the several studies may be explained by the presence of different amounts of residual water in the ionic liquid used. In order to clarify the water effect upon the spectroscopic data obtained for bmimBF_4 , an experiment was done in which different amounts of water were added to the ionic liquid: 5, 20 and 50%. Neither the Vis nor the EPR spectra show any substantial differences (see ESI†), and thus we can conclude that the coordinating ability of the neutral water molecule and the charged BF_4^- anion is very similar, and should have similar electronic effects on the central metal ion. Another possible explanation for the discrepancy found for BF_4^- in the various studies is the presence of residual chloride in the IL, since due to the miscibility of bmimBF_4

Table 3 Electronic absorption characterization of the complexes. Low energy absorption band (λ_1), difference in the 1st and 2nd absorption bands ($\lambda_{1a}-\lambda_2$), EPR anisotropy and difference in hyperfine coupling constants A_x-A_y

Ionic liquid	bbimNTf ₂	bmimNTf ₂	C ₃ OmimNTf ₂	bm ₂ imNTf ₂	bmimOTf	bmimBF ₄
λ_{1a}/nm	683	706.5	707	773	779.5	794
$\lambda_{1a}-\lambda_2/\text{nm}$	103.5	125.5	119.5	192	213.5	223
Anisotropy	Rhombic	Rhombic	Rhombic	Axial	Axial	Axial
$ A_x-A_y $ ($\times 10^4 \text{ cm}^{-1}$)	12.7	12.6	12.2	—	—	—
g_x, g_y (or g_{\perp})	1.980, 1.975	1.979, 1.974	1.979, 1.975	1.979	1.979	1.980
A_x, A_y (or A_{\perp}) ($\times 10^4 \text{ cm}^{-1}$)	54.8, 62.2	54.6, 61.9	54.6, 61.7	59.7	57.4	59.6
g_z or (g_{\parallel})	1.948	1.948	1.947	1.947	1.947	1.949
A_z (or A_{\parallel}) ($\times 10^4 \text{ cm}^{-1}$)	168.5	168.4	168.3	167.4	167.7	162.7

Ionic liquid	bmimPF ₆	bmimMeSO ₄	bmimMe ₂ PO ₄	bmimN(CN) ₂	bmimMeCO ₂
λ_{1a}/nm	682.5	786.5	826	793.5	780
$\lambda_{1a}-\lambda_2/\text{nm}$	97	204	190.5	203	190.5
Anisotropy	Rhombic	Axial	Axial	Rhombic	Axial
$ A_x-A_y $ ($\times 10^4 \text{ cm}^{-1}$)	12.2	—	—	6.9	—
g_x, g_y (or g_{\perp})	1.980, 1.974	1.979	1.976	1.976	1.977, 1.979
A_x, A_y (or A_{\perp}) ($\times 10^4 \text{ cm}^{-1}$)	55.2, 62.2	59.5	60.6	63.7	62.1, 55.2
g_z or (g_{\parallel})	1.948	1.947	1.945	1.938	1.947
A_z (or A_{\parallel}) ($\times 10^4 \text{ cm}^{-1}$)	168.5	167.4	169.7	173.8	168.2

with water it is more difficult to “wash” this IL. However, this was not evaluated since it was beyond the scope of this report.

It might seem unexpected, since the anions that are used to make ionic liquids are usually described as non-coordinating, that any difference between the ILs is seen. However, since the anions are in the neighbourhood and there is no other source of potential electron pairs as the solvent is in huge excess, they will interact with the metal centre to some extent. Hence, anions of ILs are more likely to coordinate to a transition metal centre than the same anions in a molecular solvent.

EPR spectroscopy

The VO²⁺ ion is one of the most stable diatomic cations known. When VO²⁺ is in a site of exact or near square-pyramidal symmetry, the principal directions of its g matrix are readily related to molecular axes, with the g_z (or g_{\parallel}) component coincident with the V=O bond.³⁸

The EPR spectrum of VO(acac)₂ in different organic solvents has been studied in detail by several authors.^{22,25,37–44} Many tried to correlate the experimental g values with solvent parameters, however the results suggest that coordination to the apical position is not the main influence and that solvation of the vanadyl oxygen must also be considered. It has been shown³⁷ that the magnitude of g_{\parallel} is dependent upon the energy difference $b_2(d_{xy}) \rightarrow b_1(d_{x^2-y^2})$, which varies little with the solvent. Hence, the major contribution to g comes from g_{\perp} which depends upon the energy difference between $b_2(d_{xy})$ and $e(d_{xz}, d_{yz})$ levels. These are the levels involved in the lowest energy transition, and hence the greater the energy difference between these levels, the higher the absorption energy and the smaller the magnitude of g .

The measurement of vanadium EPR spectra in ionic liquids is unexplored, however this technique is a fingerprint for equatorial coordination since the presence of different complexes in solution is detected due to the different coupling contributions of each equatorial donor group. Thus, the analysis of anisotropic EPR spectra will give detailed information on the number of species present in solution; the symmetry and coordination geometry

of the vanadium complex; and the identity of the equatorial ligands through the hyperfine coupling constant A_z (or A_{\parallel}).

For the V^{IV}O-systems Wüthrich⁴⁵ and Chasteen⁴⁶ developed an additivity rule to estimate the hyperfine coupling constant A_z^{est} [$A_z^{\text{est}} = \sum A_{z,i}$ ($i = 1$ to 4)], based on the contributions of $A_{z,i}$ of each of the four equatorial donor groups. The estimated accuracy of A_z^{est} is $\pm 3 \times 10^{-4} \text{ cm}^{-1}$. The A_z^{est} values can be used to establish the most probable binding mode in solution, however, the presence of axial donor groups isn't usually taken into account. For VO(acac)₂ type complexes, the presence of *cis* and *trans* isomers should result in two distinct sets of EPR signals with different A_z values: three oxygens from two deprotonated acac molecules and a solvent in the equatorial plane of the vanadyl ion in the first case, and four oxygen atoms in the second case.

The EPR spectra of VO(acac)₂ in some organic solvents were measured at both room temperature and 77 K (in liquid nitrogen). In a few cases aggregation resulted in a spectrum without resolution (MeCN and benzene at 77 K), in others two species were present (MeOH and EtOH). Simulation of the spectra⁴⁷ yielded the spin Hamiltonian parameters for both species found in MeOH and EtOH. One shows $A_{\parallel} = 167.6 \times 10^{-3} \text{ cm}^{-1}$ and the other $169.9 \times 10^{-3} \text{ cm}^{-1}$. The 1st one is certainly the one containing the two ligands in the equatorial position and the other probably corresponds to a complex that has a water molecule in the *cis* position—the solvents used were not previously dried and thus may contain water.

Fig. 2 shows the spectrum measured at 77 K for VO(acac)₂ dissolved in bmimOTf (and the simulated spectrum) and clearly two species are observed in solution. Thus, two complexes are present. One is the six-coordinated *trans* complex with the triflate anion occupying the 6th position, the other may be the *cis* complex with the triflate in the equatorial position and one of the CO groups axially coordinated. The *cis* isomer has been proposed for VO(acac)₂ in coordinating solvents¹² and observed by ENDOR for VO(maltol)₂ in methanol.¹⁶

In bmimMeCO₂ and bmimMe₂PO₄ two species were also found in the EPR spectra—see Fig. 3. This is in agreement with the high coordinating power of these anions and thus we

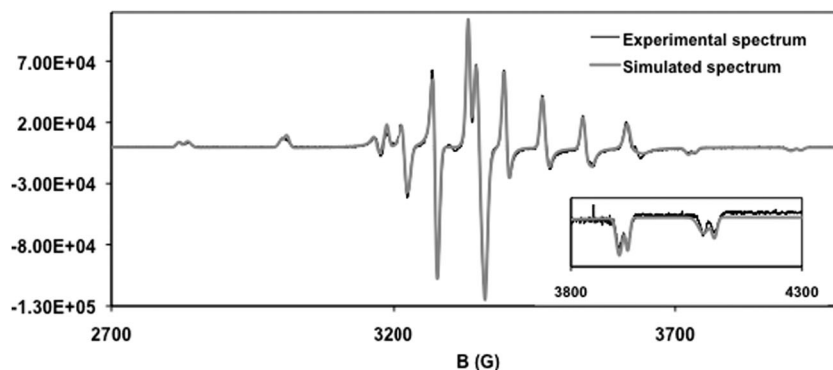


Fig. 2 EPR spectra of VO(acac)₂ in bmimOTf measured at 77 K (black) and simulated spectrum (gray).⁴⁷ Inset: high field region of the spectra showing the two species present.

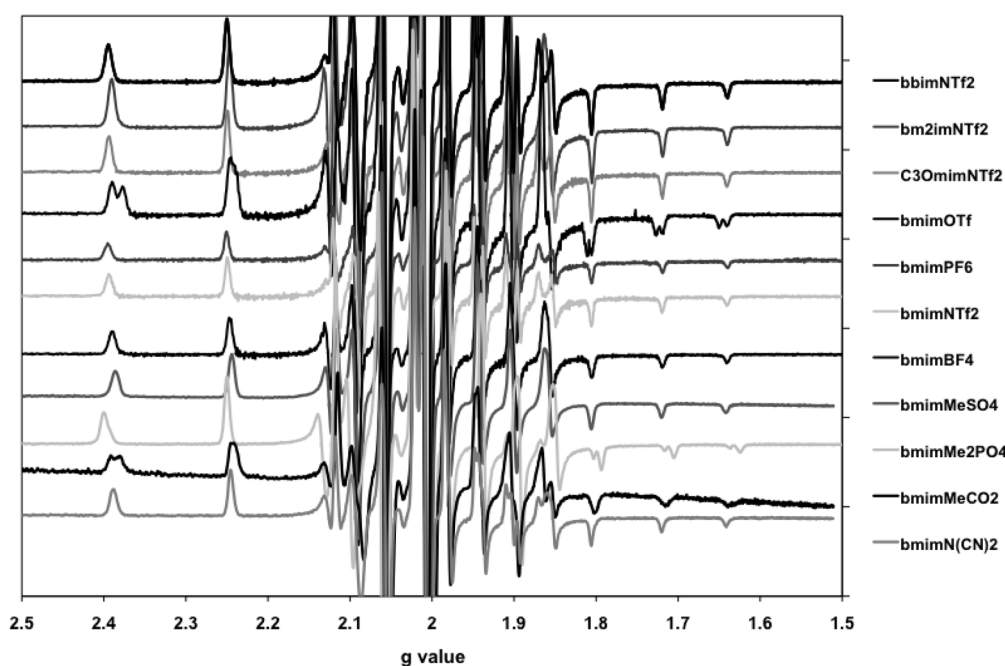


Fig. 3 EPR spectra of VO(acac)₂ measured in different ionic liquids at 77 K.

propose these to be *cis* and *trans* species. The EPR spectra measured for VO(acac)₂ in the other ionic liquids show the presence of only one species. The simulation of the spectra⁴⁷ gave the spin Hamiltonian parameters, which are collected in Table 3. The $A_{\parallel}^{\text{est}}$ for the coordination of four CO⁻ groups ($A_{\parallel}^{\text{est}} = 168.4 \times 10^{-4} \text{ cm}^{-1}$, the contribution for the carbonyl oxygen donor is $42.1 \times 10^{-4} \text{ cm}^{-1}$)⁴⁸ is in agreement with the A_{\parallel} obtained by simulation of the spectra in all ionic liquids and for the outer species in bmimOTf (see experimental data parameters in Table 3). The second species in this IL shows a lower A_{\parallel} value: $162.7 \times 10^{-4} \text{ cm}^{-1}$. We propose the following binding mode for this species: $(3 \times \text{CO}^{-}, \text{OTf}^{-})_{\text{eq}}$, which is corroborated by the DFT studies for the OTf⁻ anion (see below), considering a hydrogen bond between the bmim cation and the vanadyl oxygen.

In bmimMeCO₂ and bmimMe₂PO₄ the second isomer shows higher A_{\parallel} values. The estimated contributions of the $A_{\parallel,i}$ for the CO₂⁻ and PO₄³⁻ are 42.7×10^{-4} and $42.5 \times 10^{-4} \text{ cm}^{-1}$,⁴⁸

higher than for the CO⁻ group, and thus we propose the following binding mode for this species: $(3 \times \text{CO}^{-}, \text{An}^{-})_{\text{eq}}$.

In some ionic liquids the EPR spectra show asymmetry in the perpendicular region, presenting rhombic anisotropy. This can be interpreted in terms of a higher distortion around the metal center. The NTf₂⁻ (and PF₆⁻) ionic liquids are bulky and have high charge distribution, showing very low coordinating power, thus leaving the 6th position free. Consequently, the donor groups may shift slightly from a square pyramid to a trigonal bipyramid. In the ILs of the anions with the highest coordinating power (OTf⁻, BF₄⁻, MeSO₄⁻, MeCO₂⁻ and Me₂PO₄⁻) the EPR spectra are axial, probably due to an octahedral geometry, with the anion in the axial position. Moreover, only three bands were detected in the Vis spectra, as expected.

In bm₂imNTf₂ ionic liquid VO(acac)₂ shows axial symmetry, and therefore we can assume the coordination of the NTf₂⁻ anion in the apical position. Bm₂imNTf₂ is the ionic liquid

with the lowest hydrogen bonding ability, due to the absence of the most acidic proton at the nitrogen ring of the bm_2im^+ cation. So, we can postulate that in the ionic liquids of the other cations, which have an acidic proton, this proton is interacting with the vanadyl oxygen, lowering its electronic density. This can be compensated by coordination of an anion in the apical position or by a distortion of the geometry in order to increase the back donation from the *trans* position, for the solvents with lower coordinating power. Since this hydrogen bonding is not possible in $\text{bm}_2\text{imNTf}_2$, there is a higher drive for the anion coordination.

From the presented data we can propose that $\text{VO}(\text{acac})_2$ behaves in ionic liquids much as in organic solvents. In solvents of weak coordinating ability the complex adopts a square planar geometry in which the specific forces are dominant. This interaction is along the $\text{V}=\text{O}$ bond and therefore λ_1 and g_{\perp} are sensitive to it. In the solvents with higher power for coordination the complex adopts an octahedral geometry with an anion coordinated. In the case of bmimOTf , bmimMeCO_2 and $\text{bmimMe}_2\text{PO}_4$ two isomers are formed at 77 K, with one of them containing an anion coordinated in the *cis* position.

It is interesting to note that while the Vis electronic spectroscopy is mostly sensitive to the axial coordination, EPR spectroscopy is mostly sensitive to equatorial coordination, and while both help us to understand the picture they alone cannot explain the behavior of these complexes when dissolved in different ionic liquids. Theoretical studies by DFT were done in order to clarify the stability of the proposed species and to understand the electronic features of the system.

DFT studies

The geometry optimization of the complexes $[\text{V}(\text{=O})(\text{acac})_2]$ (**1**), *trans*-/*cis*- $[\text{V}(\text{=O})(\text{acac})_2(\text{OTf})]^-$ (*trans*-/*cis*-**[1·OTf]⁻**) and *trans*-/*cis*- $[\text{V}(\text{=O})(\text{acac})_2(\text{OTf})(\text{mmim})]$ (*trans*-/*cis*-**mmim·[1·OTf]**) ($\text{mmim} = N,N$ -dimethylimidazolium) as well as of the IL associate **[mmim]·OTf** was carried out at the B3P86 level of theory. The calculated structural parameters of **1** are in good agreement with the experimental X-ray data.⁴⁹ The maximum difference between the calculated and experimentally determined bond lengths was found for the $\text{V}=\text{O}$ bond (0.04 Å) and does not exceed 0.017 Å for other bonds, often appearing within the 3σ interval of the X-ray data.

The initial structures of *trans*-/*cis*-**mmim·[1·OTf]** (before the geometry optimization) were constructed so that the cation **[mmim]⁺** was associated with the complex molecule only *via* one H-bond with the oxo-ligand of the vanadyl group $\text{V}=\text{O}$ (Fig. 4A and B). However, as a result of the geometry optimization, the cation was shifted significantly, and a complex network of the H-bonds between **[mmim]⁺** and **[1·OTf]⁻** was created in the equilibrium structures (Fig. 4C and D). In *cis*-**mmim·[1·OTf]**, the oxo-ligand together with oxo-atoms of the acac and SO_3CF_3^- ligands participate in the H-bonding. However, in the case of *trans*-**mmim·[1·OTf]**, the vanadyl group $\text{V}=\text{O}$ does not form any H-bond with the cation-**[mmim]⁺** situated at the lateral side of the complex in respect to the $\text{V}=\text{O}$ axis. The involvement of the $\text{V}=\text{O}$ group in the

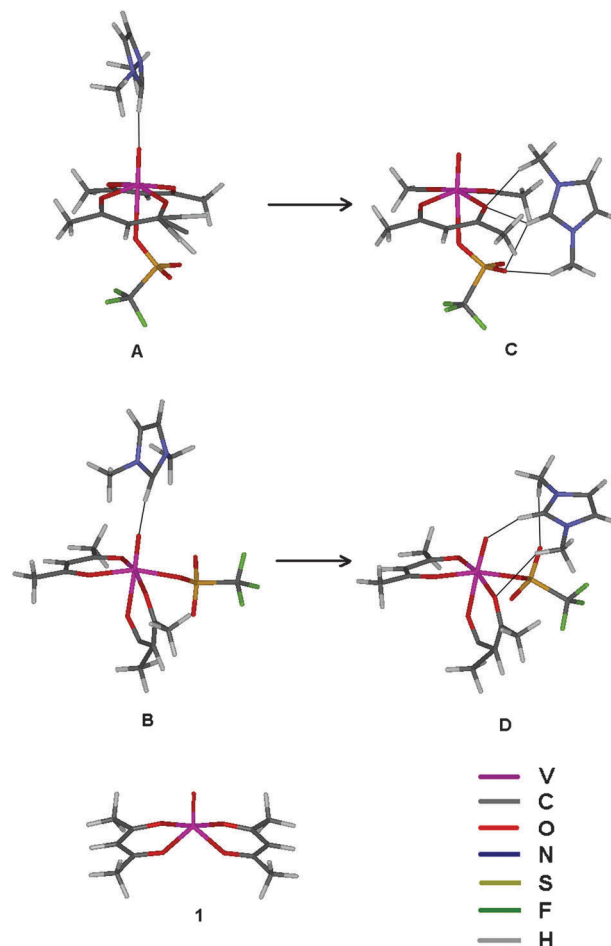


Fig. 4 Initial (A, B) and equilibrium (C, D) structures of *trans* (A, C) and *cis* (B, D) isomers of **mmim·[1·OTf]** and an equilibrium structure of **1**.

H-bonding in *cis*-**mmim·[1·OTf]** results in an elongation of this bond to 1.597 Å while that in *trans*-**mmim·[1·OTf]** it is 1.568 Å, which is similar to the value observed in complex **1** (1.561 Å). Another consequence of the association of **[mmim]⁺** to *trans*-**[1·OTf]⁻** is that the $\text{V}-\text{O}_{\text{acac}}$ bonds become non-equivalent varying from 1.977 Å to 2.022 Å in *trans*-**mmim·[1·OTf]** whereas those in **1** are equivalent (1.975 Å for the gas phase). The *trans*- $\text{O}-\text{V}=\text{O}$ fragment in *trans*-**mmim·[1·OTf]** is also slightly bent (the angle of 175.4° vs. 179.3° in *trans*-**[1·OTf]⁻**).

The calculations indicate that the triflate anion OTf^- can coordinate to the V atom, however, without consideration of the cation **[mmim]⁺**, the formed $\text{V}-\text{O}_{\text{OTf}}$ bond is rather weak. The calculated adiabatic $\text{V}-\text{O}_{\text{OTf}}$ bond energies in *trans*-**[1·OTf]⁻** and *cis*-**[1·OTf]⁻** (*i.e.*, the energies of formation of **[1·OTf]⁻** from **1** and OTf^-) are 15.4 and 9.1 kcal mol⁻¹, respectively. The consideration of the cation **[mmim]⁺** does not affect significantly the energy of formation of the associate: the reaction energies of the process **1** + **[mmim]·OTf** → **mmim·[1·OTf]** are 13.7 and 8.6 kcal mol⁻¹ for the *trans*- and *cis*-isomers, respectively. The *trans*-isomers of **[1·OTf]⁻** and **mmim·[1·OTf]** are more stable than the corresponding *cis*-isomers. The difference is 4.8 kcal mol⁻¹ (in terms of DG) for **[1·OTf]⁻** but only 1.9 kcal mol⁻¹ for **mmim·[1·OTf]**.

The latter small value explains the experimental detection of both isomers in solution.

The calculated values of the hyperfine coupling constants $|A_z|$, $|A_y|$ and $|A_x|$ for complexes *trans*-/*cis*-[1-OTf]⁻ are 167.3×10^{-4} , 66.1×10^{-4} and $59.4 \times 10^{-4} \text{ cm}^{-1}$ for the *trans*-isomer and 172.6×10^{-4} , 71.7×10^{-4} and $69.0 \times 10^{-4} \text{ cm}^{-1}$ for the *cis*-isomer. The consideration of the cation association in complexes **mmim**·[1-OTf] results in the $|A_z|$, $|A_y|$, and $|A_x|$ values of 166.3×10^{-4} , 65.4×10^{-4} and $58.8 \times 10^{-4} \text{ cm}^{-1}$ (*trans*-isomer) and 162.3×10^{-4} , 61.1×10^{-4} and $56.7 \times 10^{-4} \text{ cm}^{-1}$ (*cis*-isomer). The hyperfine tensor has an axial symmetry and the direction of A_z coincides with the V = O bond. The perpendicular tensors are directed between the equatorial donor atoms. The calculations indicate that in the case of **mmim**·[1-OTf] the higher values of $|A_z|$ correspond to the *trans*-isomers while the situation is opposite for [1-OTf]⁻. The computational data obtained for **mmim**·[1-OTf] are in better agreement with the experimental results. Indeed, two isomers were found by EPR spectroscopy in bmimOTf with A_z values of 167.7×10^{-3} and $162.7 \times 10^{-3} \text{ cm}^{-1}$, which we tentatively assigned to *trans* and *cis* isomers, respectively. In the other ionic liquids only one species was observed which we assigned to the *trans* isomer. The DFT studies corroborate these assignments and show that the explicit inclusion of the **mmim**⁺ cation in the calculations is critical for the correct predictions of the EPR parameters.

Conclusions

The spectroscopic studies presented in this paper show that VO(acac)₂ is a very good solvatochromic probe in ionic liquids enabling the establishment of the following basicity order: PF₆⁻ < NTf₂⁻ < OTf⁻ ≈ MeCO₂⁻ < MeSO₄⁻ < BF₄⁻ ≈ N(CN)₂⁻ < Me₂PO₄⁻, in agreement with determinations of other authors with different metal probes.

The EPR spectroscopic characterization showed the presence of two species coexisting in solution, in bmimOTf, bmimMeCO₂ and bmimMe₂PO₄. The *trans* complex is the most important one in all the studied ionic liquids except bmimOTf, bmimMeCO₂ and bmimMe₂PO₄ where coordination of the anion in the equatorial position was also observed. Although the LSER correlations done with the Vis data in ionic liquids present a low correlation parameter, they evidence the influence of the β Kamlet–Taft parameter on the solvation of VO(acac)₂. The DFT studies show the higher stability of the *trans* isomers (when compared to the *cis*) and confirmed the importance of the hydrogen bond donating ability from the cation, showing that the hyperfine coupling constant A_z for the *cis* isomer changes more than $10 \times 10^{-4} \text{ cm}^{-1}$ upon consideration of the cation association to the VO(acac)₂OTf complex.

The results clearly show how the choice of ionic liquid may lead to differences in the solvation forces and thus the structure of the catalyst in solution. This may affect profoundly the catalyst performance and activity.

Studies are underway in order to evaluate the reactivity of these systems in the oxidative desulfurization of fuels. This might lead to interesting structure/activity relationships that will help us build more efficient and consequently sustainable processes.

Experimental

Materials and reagents

All chemicals used were of analytical reagent grade. 1-Methylimidazole was purchased from Acros Organics and distilled from potassium hydroxide; 1-chlorobutane was purchased from Acros Organics and distilled from phosphorus pentoxide. Lithium bis(trifluoromethylsulfonyl)imide [Li(NTf₂)] and lithium trifluoromethanesulfonate [Li(OTf)] were purchased from Apollo Scientific and used as received. Bis(acetylacetonate)-vanadium(IV) was also obtained from Acros Organics. All syntheses and sample preparations were performed under anaerobic conditions using standard Schlenk techniques. The preparation and spectral data of the ionic liquids have been described elsewhere.²³

Instruments

¹H NMR spectra were recorded on a Bruker 300 or 400 MHz spectrometer. UV-vis spectra were recorded on a Perkin-Elmer UV-visible Lambda 35 spectrophotometer and the temperature was controlled with a Peltier controller from Perkin-Elmer. The EPR spectra were recorded at 77 K (on glasses made by freezing solutions in liquid nitrogen) and some at room temperature with a Bruker ESP 300E X-band spectrometer.

LSER

The error associated with each parameter in eqn (1) was appraised in terms of the *p*-value, and any terms found to be statistically insignificant were eliminated. Only where an acceptable *p*-value for the coefficients *a*, *b* and *s* is found is the result shown. It was decided to take as acceptable only those parameters whose statistically significant *p*-value does not exceed the limit level of 0.05.

Vis spectra

The visible electronic spectra were measured in THF, acetone, dichloroethane, isopropanol, ethyl acetate, dichloromethane, methanol, ethanol, DMSO, DMF, benzene and acetonitrile. The samples were prepared under nitrogen with Schlenk techniques to avoid vanadium oxidation, however the organic solvents used were not previously dried. The VO(acac)₂ concentration used was ca. 5 mM.

Computational details

The full geometry optimization of all structures was carried out at the DFT level of theory (unrestricted approximation) using B3P86^{50,51} functional with the help of the Gaussian-03⁵² program package. This functional was found to be appropriate for the theoretical studies of V complexes, e.g. those with Schiff bases.⁵³ No symmetry operations have been applied for any of the structures calculated. The standard 6-31G(d) basis set was used for all atoms. The Hessian matrix was calculated analytically for all optimized structures in order to prove the location of correct minima (no imaginary frequencies) and to estimate the thermodynamic parameters, the latter being calculated at 25 °C. The ⁵¹V hyperfine coupling constants were estimated at the single-point calculations using the BH and HLYP functional and the 6-311G* basis set for all

atoms on the basis of the equilibrium geometries obtained at the B3P86/6-31G* level of theory. The anisotropic ^{51}V hyperfine coupling constants A_x , A_y , and A_z were estimated as the sum of the isotropic Fermi contact term and the corresponding dipolar hyperfine interaction term.⁵⁴ The stability test was performed for all structures using the keyword STABLE in Gaussian-03.

Acknowledgements

The work was financially supported by Fundação para a Ciência e Tecnologia (project PTDC/QUI-QUI/098516/2008).

References

- 1 T. Welton, *Chem. Rev.*, 1999, **99**, 2071–2083.
- 2 L. Crowhurst, N. L. Lancaster, J. M. Perez-Arlandis and T. Welton, *Ionic Liquids Iib: Fundamentals, Progress, Challenges and Opportunities: Transformations and Processes*, 2005, vol. 902, pp. 218–232.
- 3 Y. Chauvin, L. Mussmann and H. Olivier, *Angew. Chem., Int. Ed.*, 1996, **34**, 2698–2700.
- 4 P. Wasserscheid, C. M. Gordon, C. Hilgers, M. J. Muldoon and I. R. Dunkin, *Chem. Commun.*, 2001, 1700.
- 5 C. Reichardt, *Solvents and Solvent Effects in Organic Chemistry*, Wiley-VCH Verlag GmbH & Co. KGaA, Weinheim, 3rd edn, 2004.
- 6 M. J. Muldoon, C. M. Gordon and I. R. Dunkin, *J. Chem. Soc., Perkin Trans. 2*, 2001, 433–435.
- 7 R. Lungwitz, M. Friedrich, W. Linert and S. Spange, *New J. Chem.*, 2008, **32**, 1493–1499.
- 8 J. Bartosik and A. V. Mudring, *Phys. Chem. Chem. Phys.*, 2010, **12**, 4005–4011.
- 9 S. Pitula and A. V. Mudring, *Phys. Chem. Chem. Phys.*, 2010, **12**, 7056–7063.
- 10 I. Persson, *Pure Appl. Chem.*, 1986, **58**, 1153–1161.
- 11 C. H. Ahlers and C. P. J. Vanvuuren, *Thermochim. Acta*, 1989, **145**, 353–355.
- 12 S. S. Amin, K. Cryer, B. Y. Zhang, S. K. Dutta, S. S. Eaton, O. P. Anderson, S. M. Miller, B. A. Reul, S. M. Brichard and D. C. Crans, *Inorg. Chem.*, 2000, **39**, 406–416.
- 13 D. C. Crans, S. S. Amin, K. Cryer, B. Y. Zhang, S. S. Eaton and O. P. Anderson, *Abstr. Pap. Am. Chem. Soc.*, 1999, **217**, U1043.
- 14 R. Grybos, A. Samotus, N. Popova and K. Bogolitsyn, *Transition Met. Chem.*, 1997, **22**, 61–64.
- 15 H. Vanwilligen, *Chem. Phys. Lett.*, 1979, **65**, 490–493.
- 16 D. Mustafi and M. W. Makinen, *Inorg. Chem.*, 2005, **44**, 5580–5590.
- 17 W. Linert, E. Herlinger, P. Margl and R. Boca, *J. Coord. Chem.*, 1993, **28**, 1–16.
- 18 R. P. Dodge, A. Zalkin and D. H. Templeton, *J. Chem. Phys.*, 1961, **35**, 55–67.
- 19 A. K. Gregson and S. Mitra, *Inorg. Chim. Acta*, 1980, **45**, L121–L122.
- 20 J. S. Hwang and M. H. Rahman, *Abstr. Pap. Am. Chem. Soc.*, 1991, **202**, 264-PHYS.
- 21 D. C. Crans, *J. Inorg. Biochem.*, 2000, **80**, 123–131.
- 22 E. Garribba, G. Micera and D. Sanna, *Inorg. Chim. Acta*, 2006, **359**, 4470–4476.
- 23 L. Cammarata, S. G. Kazarian, P. A. Salter and T. Welton, *Phys. Chem. Chem. Phys.*, 2001, **3**, 5192–5200.
- 24 A. Urbanczyk and M. K. Kalinowski, *Monatsh. Chem.*, 1983, **114**, 1311–1319.
- 25 I. Bernal and P. H. Rieger, *Inorg. Chem.*, 1963, **2**, 256–260.
- 26 J. Selbin and T. R. Ortolano, *J. Inorg. Nucl. Chem.*, 1964, **26**, 37–40.
- 27 A. Urbanczyk and M. K. Kalinowski, *Monatsh. Chem.*, 1990, **121**, 879–881.
- 28 C. J. Ballhausen and H. B. Gray, *Inorg. Chem.*, 1962, **1**, 111–122.
- 29 M. J. Kamlet, J. L. Abboud and R. W. Taft, *J. Am. Chem. Soc.*, 1977, **99**, 6027–6038.
- 30 M. J. Kamlet and R. W. Taft, *J. Am. Chem. Soc.*, 1976, **98**, 377–383.
- 31 R. W. Taft and M. J. Kamlet, *J. Am. Chem. Soc.*, 1976, **98**, 2886–2894.
- 32 T. Yokoyama, R. W. Taft and M. J. Kamlet, *J. Am. Chem. Soc.*, 1976, **98**, 3233–3237.
- 33 L. Crowhurst, N. L. Lancaster, J. M. P. Arlandis and T. Welton, *J. Am. Chem. Soc.*, 2004, **126**, 11549–11555.
- 34 C. P. Fredlake, M. J. Muldoon, S. N. V. K. Aki, T. Welton and J. F. Brennecke, *Phys. Chem. Chem. Phys.*, 2004, **6**, 3280–3285.
- 35 L. Crowhurst, P. R. Mawdsley, J. M. Perez-Arlandis, P. A. Salter and T. Welton, *Phys. Chem. Chem. Phys.*, 2003, **5**, 2790–2794.
- 36 Y. Marcus, *Chem. Soc. Rev.*, 1993, **22**, 409–416.
- 37 C. M. Guzy, J. B. Raynor and M. C. R. Symons, *J. Chem. Soc. A*, 1969, 2791–2795.
- 38 D. Kivelson and S. Lee, *J. Chem. Phys.*, 1964, **41**, 1896–1903.
- 39 F. A. Walker, R. L. Carlin and P. H. Rieger, *J. Chem. Phys.*, 1966, **45**, 4181–4189.
- 40 R. L. Carlin and F. A. Walker, *J. Am. Chem. Soc.*, 1965, **87**, 2128–2133.
- 41 C. P. Stewart and A. L. Porte, *J. Chem. Soc., Dalton Trans.*, 1972, 1661–1666.
- 42 N. M. Atherton, P. J. Gibbon and M. C. B. Shohoji, *J. Chem. Soc., Dalton Trans.*, 1982, 2289–2290.
- 43 N. S. Angerman and R. B. Jordan, *J. Chem. Phys.*, 1971, **54**, 837–843.
- 44 M. Patron, D. Kivelson and R. N. Schwartz, *J. Phys. Chem.*, 1982, **86**, 518–524.
- 45 K. Wüthrich, *Helv. Chim. Acta*, 1965, **48**, 1012–1017.
- 46 N. D. Chasteen, *Biological Magnetic Resonance*, Plenum, New York, 1981, vol. 3, pp. 53–119.
- 47 A. Rockenbauer and L. Korecz, *Appl. Magn. Reson.*, 1996, **10**, 29–43.
- 48 T. S. Smith, R. LoBrutto and V. L. Pecoraro, *Coord. Chem. Rev.*, 2002, **228**, 1–18.
- 49 M. Hoshino, A. Sekine, H. Uekusa and Y. Ohashi, *Chem. Lett.*, 2005, **34**, 1228–1229.
- 50 A. D. Becke, *J. Chem. Phys.*, 1993, **98**, 5648–5652.
- 51 C. T. Lee, W. T. Yang and R. G. Parr, *Phys. Rev. B*, 1988, **37**, 785–789.
- 52 G. W. Frisch, H. B. Schlegel, G. E. Scuseria, M. A. Robb, J. R. Cheeseman, J. A. Montgomery, Jr, T. Vreven, K. N. Kudin, J. C. Burant, J. M. Millam, S. S. Iyengar, J. Tomasi, V. Barone, B. Mennucci, M. Cossi, G. Scalmani, N. Rega, G. A. Petersson, H. Nakatsuji, M. Hada, M. Ehara, K. Toyota, R. Fukuda, J. Hasegawa, M. Ishida, T. Nakajima, Y. Honda, O. Kitao, H. Nakai, M. Klene, X. Li, J. E. Knox, H. P. Hratchian, J. B. Cross, C. Adamo, J. Jaramillo, R. Gomperts, R. E. Stratmann, O. Yazyev, A. J. Austin, R. Cammi, C. Pomelli, J. W. Ochterski, P. Y. Ayala, K. Morokuma, G. A. Voth, P. Salvador, J. J. Dannenberg, V. G. Zakrzewski, S. Dapprich, A. D. Daniels, M. C. Strain, O. Farkas, D. K. Malick, A. D. Rabuck, K. Raghavachari, J. B. Foresman, J. V. Ortiz, Q. Cui, A. G. Baboul, S. Clifford, J. Cioslowski, B. B. Stefanov, G. Liu, A. Liashenko, P. Piskorz, I. Komaromi, R. L. Martin, D. J. Fox, T. Keith, M. A. Al-Laham, C. Y. Peng, A. Nanayakkara, M. Challacombe, P. M. W. Gill, B. Johnson, W. Chen, M. W. Wong, C. Gonzalez and J. A. Pople, *Gaussian 03, revision D.01*, Gaussian, Inc., Wallingford CT, 2004.
- 53 M. R. Maurya, A. Arya, A. Kumar, M. L. Kuznetsov, F. Avicella and J. C. Pessoa, *Inorg. Chem.*, 2010, **49**, 6586–6600.
- 54 S. Gorelsky, G. Micera and E. Garribba, *Chem.–Eur. J.*, 2010, **16**, 8167–8180.